Supplementary Information

Coming across a novel copper oxide 2D framework during the oxidation of Cu(111)

Sonia Matencio,[†] Esther Barrena and Carmen Ocal*

Institut de Ciència de Materials de Barcelona (ICMAB-CSIC)
Campus de la UAB, 08193 Bellaterra, Spain.

* Corresponding author
Email: cocal@icmab.es

[†] Present address: Institute of Experimental and Applied Physics, University of Regensburg, 93053 Regensburg, Germany

Clean Cu(111): STM, LEED and XPS

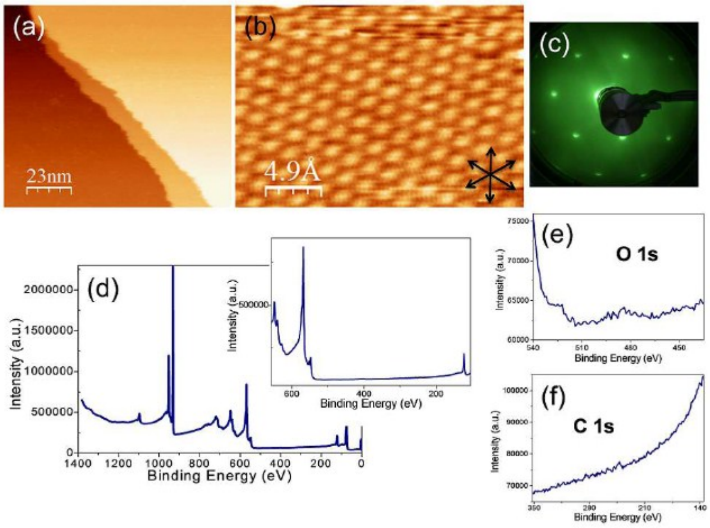

Figure SI1. Clean Cu(111) surface. Large (a) and small (b) topographic STM images: The monoatomic steps ($d_{Cu(111)}$ = 2.1 Å) in the large scale areas and the atomic resolution in small scans ($a_{Cu(111)}$ = 2.56 Å) were used for XY and Z scanner calibration to accurately determine the lattice parameters of the oxide structures. STM parameters: (a) I= 375 pA, Bias = – 1.40 V and (b) I= 240 pA, Bias = – 0.30 V. The arrows in (b) indicate the <111> directions of the Cu(111). (c) LEED pattern of the clean Cu(111). It served to check cleanness but also to univocally determine the relative orientation between the substrate and the different oxide lattices. After substrate cleaning, the XPS survey (d), O1s (e) and C1s (f) indicated no important traces of contaminants.

Air-enriched Ar gas

Ambient air was introduced by means of a leak valve through the same pipe that the Ar gas, to the Ultra-High-Vacuum (UHV) preparation chamber. The pressure in the UHV chamber during oxidation was kept in the 10^{-5} mbar range and the gas mixture was ionized with the ion gun. The spectra corresponding to the residual gas analyzer (RGA) signal for a pressure of 10^{-6} mbar is shown in the figure. The peaks assignment is given in the figure caption.

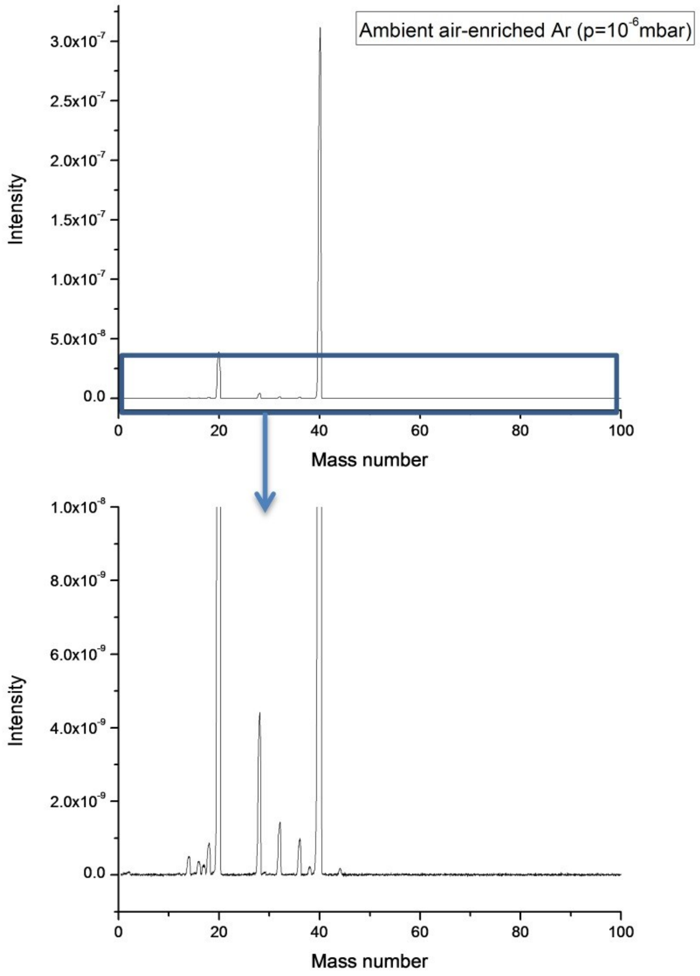

Figure SI2. Spectra of the residual gas in the preparation chamber during the entrance of ambient air-enriched Ar ($P = 10^{-6}$ mbar). The main gas constituents are identified in the magnified spectrum as: Ar (20, 40), H_2O (group 16-18), N_2 (28) and O_2 (32)

Oxygen adsorption on Cu(111)

The adsorption of oxygen atoms on the Cu(111) has been observed both, after exposure to O_2 at RT[1] and in the last stages of $Cu_2O(111)$ reduction by CO.[2] Appearing either as isolated oxygen species or small oxygen clusters on the Cu(111) terraces, they are seen as depressions surrounded by concentric rings in the high resolution constant current STM images of Figure SI3, but as dark or bright spots depending on tip conditions. These rings correspond to oscillations (standing waves) in the electronic density of states of the cooper surface due to the oxygen adsorption (Friedel's oscillations). The adsorption site of the O atoms was determined to be threefold hollow[1] from atomically resolved STM images. As it can be seen in Figure SI3b-c, these oxygen species can be moved by the sweep action of the tip during STM, indicating a weakly interaction with the unreconstructed substrate. This oxygen does not react at the copper terraces neither importantly attaches to the step edges. Thus, for instance the frizzy appearance of some steps is a clear indication of the metal atoms diffusion along oxygen free step edges.[3,4] The double height seen at some of the steps points to the beginning of oxidation described in the main text.

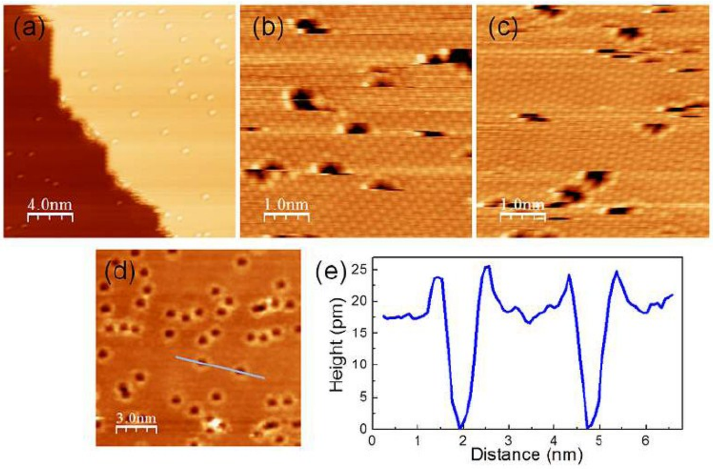

Figure SI3. Large scale topographic STM image of oxygen adsorbed in the Cu(111) surface (a). The high resolution images in (b) and (c) correspond to consecutive scans in the same area. A non-negligible drift during scan down (b) and up (c) is accompanied by a tip induced motion of the oxygen species. A medium scale image in (d) and the corresponding line profile (e) illustrate that these species are imaged as holes 15-20 pm deep and an apparent diameter of ~1 nm. STM parameters: (a-d) I = 240 pA, Bias = – 0.30 V.

Short order honeycomb (5-7 defects) and O-deficient structures

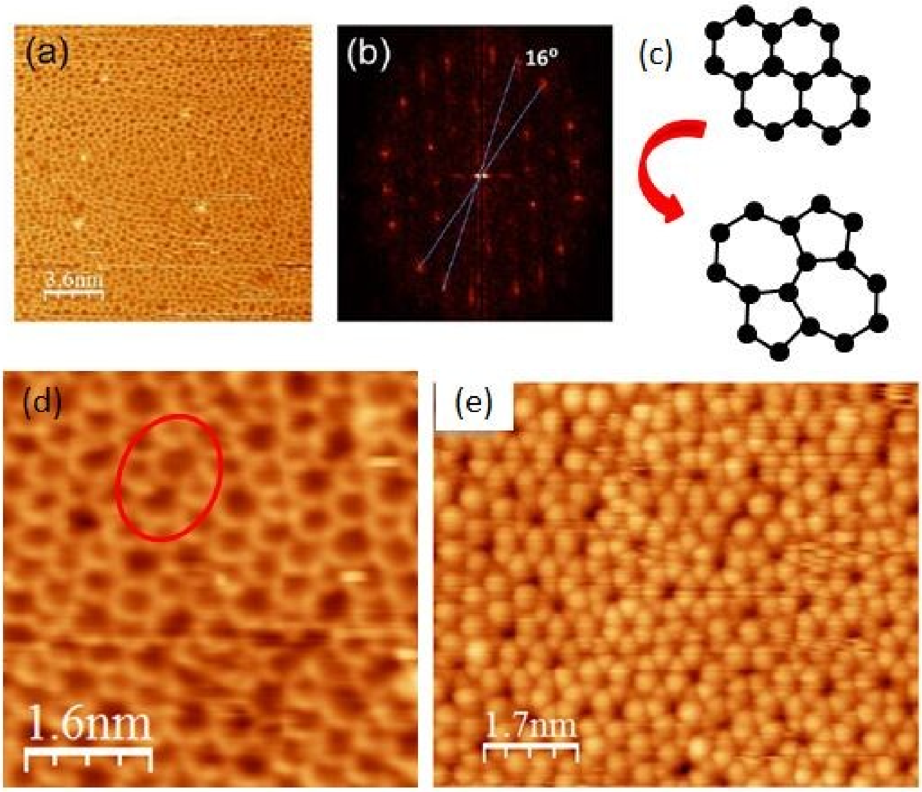

Figure SI4. (a, d, e) STM images of the defective or short order range honeycomb structure. Pentagons and heptagons are seen embedded in the honeycomb lattice (red circle in (d)). These topological 5-7 defects have been proposed to be analogous to the Stone-Wales (S-W) defects occurring, for instance, in graphene[5,6] and are generated by 90° rotation of bonds about the midpoint.[7] Each oxide unit forming the lattice is depicted as a block dot in the schematic model of (c). Depending on the imaging resolution, the individual units could be seen (e).[8] STM parameters: (a, d) I = 194 pA, Bias = – 0.47 V, (e) I = 80 pA, Bias = – 0.53 V.

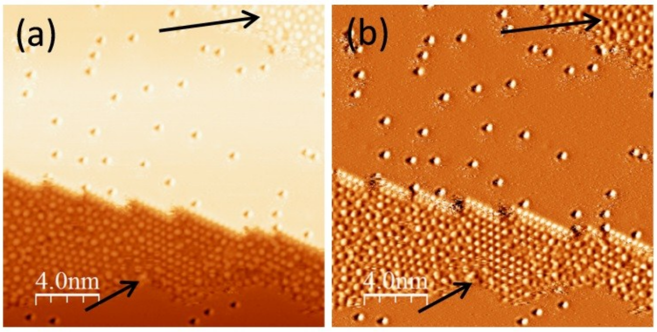

Figure SI5. STM topographic (a) and current (b) images of the O-deficient oxide structure at the edges of two consecutive substrate terraces. STM parameters: (a) I = 175 pA, Bias = + 1.70 V. *Note the nearly perfect hexagonal array formed by grouped neighboring oxygen vacancies.*

Dependence of the “44” structure on imaging conditions

Copper oxide STM images have been found to be strongly bias and tip conditions dependent. This is illustrated here by showing STM topographic images of the same “44” oxide structure at different tip and tunneling conditions. An impressive variation on the superlattice appearance is observed. Figure SI6a (Figure 4b in the main text) shows the honeycomb array result of a high resolution imaging with faint triangular groups of brighter/darker hexagons. The lattice is formed by bright dots in Figure SI6b which appear broadened forming a compact close packed lattice (~ 6 Å) in Figures SI6c and 6d. These two later were found to transform the one into the other during scanning as illustrated in the bottom panels of the Figure. The arrows indicate the sense of fast scan direction. These changes can be only attributed to tip modifications during scanning (green to red arrows) and probably correspond to a tip with an adsorbate at the apex.

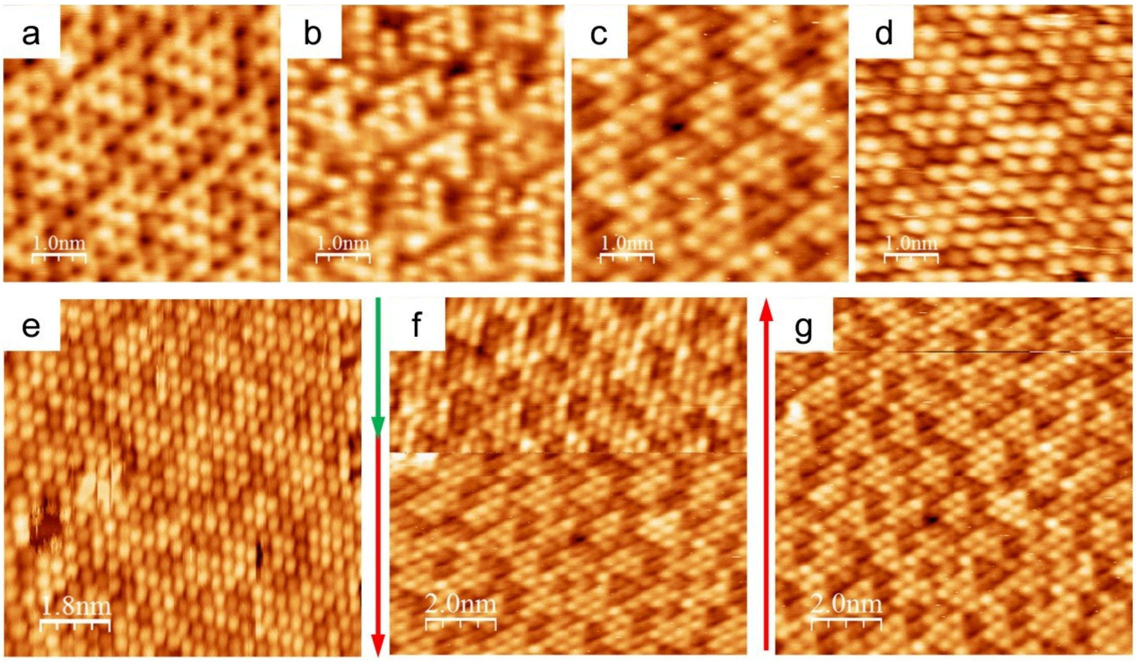

Figure SI6. Top: STM topographic images of the non-stoichiometric “44” structure obtained at three different tip conditions. (e)-(g) Consecutive STM images where the arrows indicate the fast scan direction. The arrow color change in (f) signals the point where resolution changes due to tip modification during scanning. STM parameters: (a) I = 100 pA, Bias = + 0.97 V, (b) I = 126 pA, Bias = + 1.20 V, (c) I = 338 pA, Bias = – 1.20 V, (d)-(e) I = 180 pA, Bias = + 0.97 V, (f)-(g) I = 340 pA, Bias = + 1.17 V.

Coincidence lattice and Moiré patterns

In addition to the bias and tip conditions dependence in STM and the easy occurrence of both, topological and stoichiometric defects, copper oxides imaging is quite troublesome because the large misfit between the oxide layer and the substrate leads, in practice, to similar but not identical surface structures and, commonly, site coincident lattice (SCL) or Moiré-like patterns can be observed. In these patterns, equivalent atoms of the overlayer adopt different sites on top of the substrate, therefore, exhibiting both a different local height reflected in true topographic differences and a different local density of stated (LDOS), this fact is reflected in a bias dependence. One of the proposed models to interpret such superstructures observed for the "44" is presented in Figure SI7a (drawing adapted from ref. 9) as a superlattice with a coincidence boundary at the $Cu_2O(111)/Cu(111)$ interface. The oxide layer (oxide units represented by green dots) is strained to adopt the large misfit with the substrate. As three times of the overgrowth periodicity (3×5.95 Å =17.85 Å) nearly equals seven times the NN distance of the Cu substrate (7×2.56 Å = 17.92 Å), the SCL described by the large oblique unit cell (dashed red line in the figure) is 9 times the oblique Cu_2O unit cell (small rhomboid) and can be identified in Wood's notation by a $(7\sqrt{3}x7\sqrt{3})R30^{o}$ or $c(7x7\sqrt{3})$ superstructure of the Cu(111) (rectangular unit cell). Depending on the relative orientation between overlayer and substrate many different patterns may exist for the same overlayer structure (e.g., archetypical graphene Moiré patterns on (111) oriented metals). In the particular case of the copper oxide overlayers, the situation becomes even more complex. An experimentally observed $Cu_2O(111)$-like or "44" structure and the corresponding Fast Fourier Transform (FFT) are presented in Figure SI7b and SI7c, respectively. As it can be observed in the FFT, two concentric hexagonal lattices can be distinguished, the outermost pattern having a 7 times larger periodicity than the inner pattern. The separated respective FFTs and the inverse FFTs (IFFTs) are also shown (Figure SI6d-g). The hexagonal lattice in Figures SI7d and SI7f corresponds to the characteristic ~ 6 Å distance of the Cu_2O, while the large lattice is result of the large superstructure of this example.

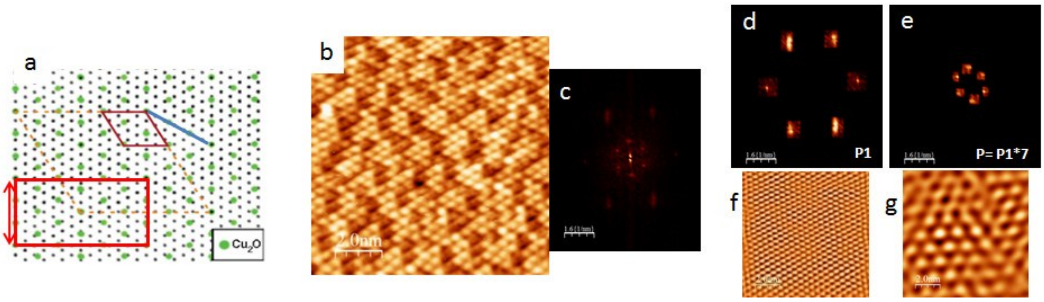

Figure SI7. (a) Model for a coincident site lattice of the $Cu_2O(111)$-"44" structure on Cu(111).[10, 11] For simplicity, green dots stand for oxide units forming the oxide layer and black small dots represent the underlying substrate (drawing adapted from ref. 9). Depicted unit cells are described in the text. (b) Topographic STM image of the non-stoichiometric "44" structure and (c) corresponding FFT. (d) and (e) are the separated hexagonal lattices of (c) and (f) and (g) the corresponding inverse FFTs. STM parameters: (b) I = 340 pA, Bias = +1.17 V.

Coexistence of oxide layers with different oxygen content

As commented in the main manuscript, all observed structures coexist on one or other regions.

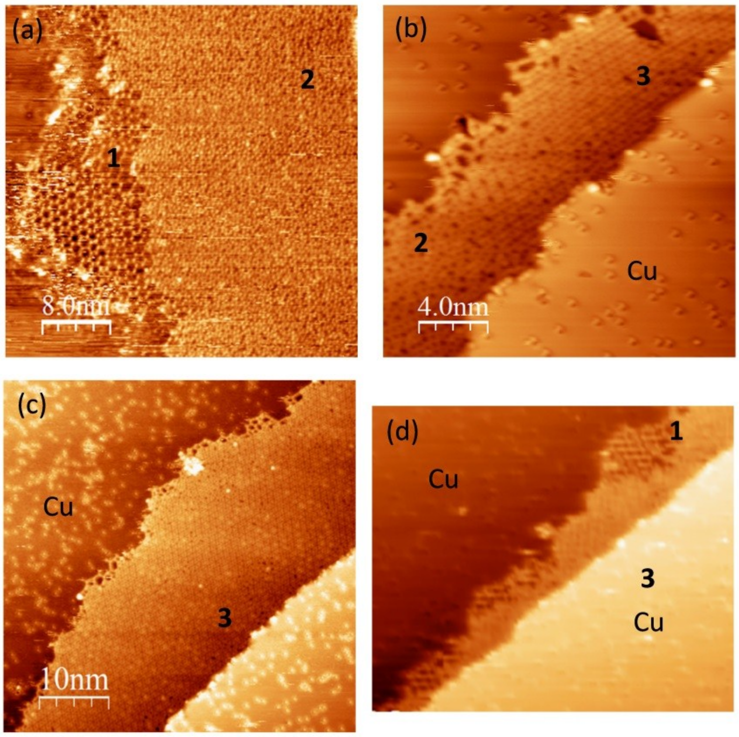

Figure SI8. STM images of the partially oxidized Cu(111) showing that the different structures described in the main text coexist on the surface. Increasing numbers labeling the structures indicate increasing oxygen content: (1) open honeycomb (OHC), (2) short order honeycomb (SOHC) and (3) compact “44” or $Cu_2O(111)$-like. STM parameters: (a) = 94 pA, Bias = – 0.90 V, (b) I = 187 pA, Bias = – 1.40 V, (c) I = 62 pA, Bias = –1.40 V, (d) I = 117 pA, Bias = – 1.40 V.

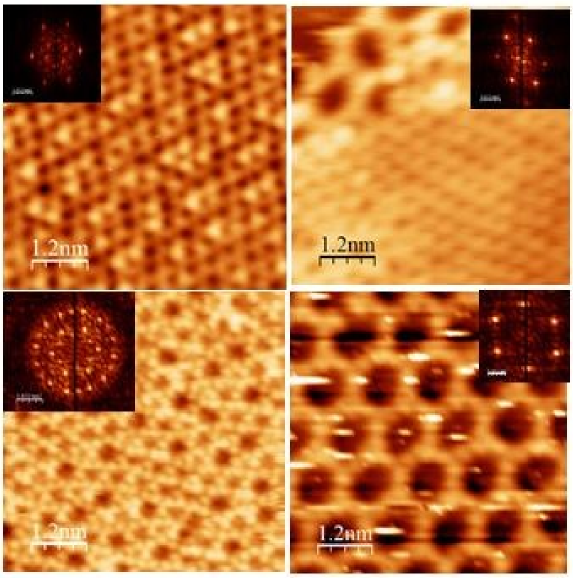

Figure SI9. High resolution STM images of the different oxide structures and their corresponding Fast Fourier Transforms (FFT).

Residual incorporation of nitrogen

It has been reported that nitrogen does not chemisorbed on copper directly unless this process is activated by ion implantation or atomic beam sources. Though the ionization energy for nitrogen is higher than for oxygen, nitrogen ionized species would exist during the air-enriched procedure employed in the present investigation.

Previous studies on the incorporation of nitrogen in Cu(111) indicate that the ordered structure experimentally observed is a pseudo-(100) surface phase with a rectangular unit cell. [11-15] As demonstrated by DFT calculations, [16] this structure is highly energetically favorable. Though scarcely, we observed small surface regions (Figure SI10) presenting a surface structure in agreement with copper nitride formation. This CuN layer has been interpreted by insertion nitrogen atoms between Cu atoms in the surface. Because the insulating character of the nitride layer, in the constant current STM images of Figure SI10, it appears lower than the level of the original Cu terrace (see profile in d). The difference in height depending on the measuring parameters.[15] The nitride lattice has a (25×7√3)rect unit cell well known, clearly identifiable and distinguishable from all the hexagonal and honeycomb structures developed during copper oxide formation.

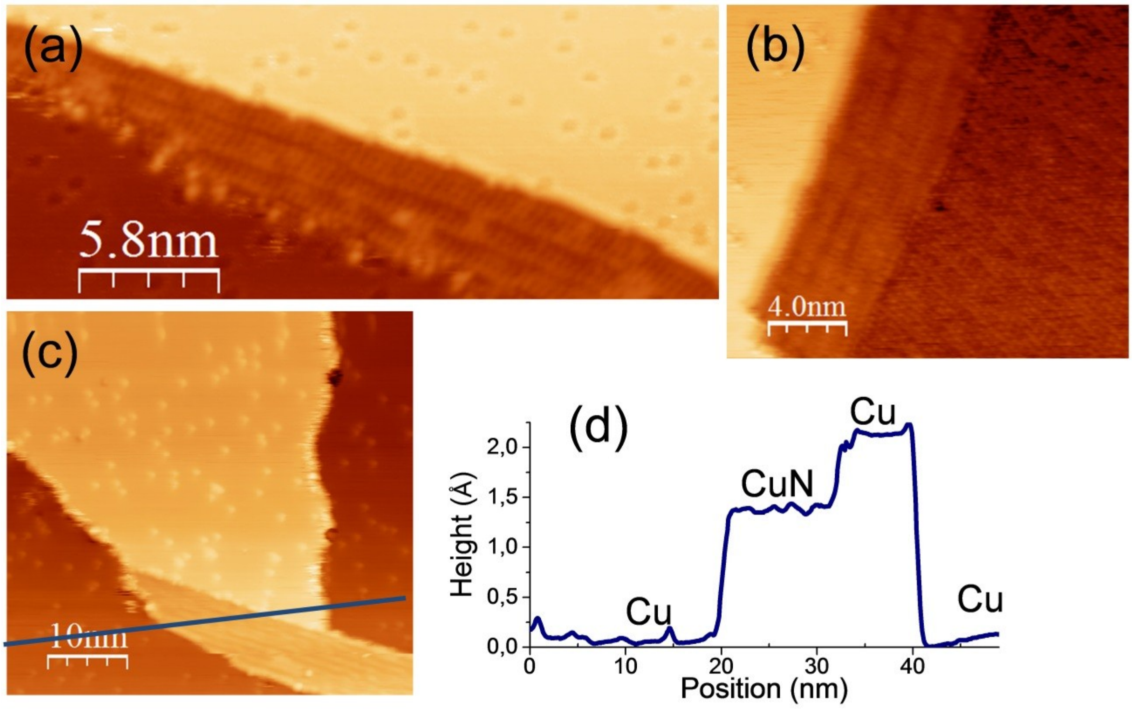

Figure SI10. STM images of a region of a Cu(111) where residual incorporation of nitrogen is observed. STM parameters: I = 200pA, Bias = – 0.80V. The images reveal the (25×7√3)rect. coincidence surface mesh resulting from pseudo-(100) layer and the underlying (111) substrate. The modulation or regular wavy bands running along close-packed <110> directions of the substrate characteristic of the coincidence mesh are accompanied for a small angular distortion ($\phi \approx 14°$ in our case) of the CuN super cell away from the <110> direction of Cu substrate results in a long-range modulation disorder.[15]

REFERENCES

(1) F. Wiame, V. Maurice, P. Marcus. Initial stages of oxidation of Cu(111). Surface Science, 601(5), 1193-1204, 2007

(2) F. Yang, Y. Choi, P. Liu, J. Hrbek, J. A. Rodriguez. Autocatalytic Reduction of a Cu_2O/Cu(111) Surface by CO: STM, XPS, and DFT Studies. The Journal of Physical Chemistry C, 114(40), 17042-17050, 2010

(3) M. Giesen-Seibert, R. Jentjens, M. Poensgen, and H. Ibach. Time dependence of step fluctuations on vicinal Cu(1119) surfaces investigated by tunneling microscopy. Physical Review Letters, 71(21):3521-3525, 1993

(4) M. Giesen-Seibert, F. Schmitz, R. Jentjens, and H. Ibach. Time fluctuations of steps on Cu(11n) surfaces investigated by temperature variable tunneling microscopy. Surface Science, 329(1-2):47-60, 1995

(5) A. Hashimoto, K. Suenaga, Al. Gloter, K. Urita, and S. Iijima. Direct evidence for atomic defects in graphene layers. Nature, 430(7002):870-873,2004.

(6) J. C. Meyer, C. Kisielowski, R. Erni, M. D. Rossell, M. F. Crommie, and A. Zettl. Direct imaging of lattice atoms and topological defects in graphene membranes. Nano Letters, 8(11):3582-3586, 2008.

(7) G. Rajasekaran and Avinash Parashar. Molecular dynamics study on the mechanical response and failure behaviour of graphene: performance enhancement via 5–7–7–5 defects. RSC Adv., 2016, 6, 26361–26373.

(8) F. Yang, Y. Choi, P. Liu, D. Stacchiola, J. Hrbek, J. A. Rodriguez. Identification of 5 -7 Defects in a Copper Oxide Surface. Journal of the American Chemical Society, 133, 11474-11477, 2011.

(9) C. Pérez- León, C. Sürgers, H. V. Löhneysen. Formation of copper oxide surface structures via pulse injection of air onto Cu(111) surfaces. Phys. Rev. B, 85(3),035434, 2012.

(10) J. H. Ho and R. W. Vook, (111)Cu_2O growth modes on (111)Cu surfaces J. Crystal Growth **44**, 561 (1978).

(11) F. Jensen, F. Besenbacher, E. Lægsgaard, and I. Stensgaard, Oxidation of Cu(111): two new oxygen induced reconstructions. Surf. Sci. **259**, L774 (1991).

(12) S.M. Driver, Ph Woodruff. Nitrogen-induced pseudo-(100) reconstruction of the Cu(111) surface identified by STM. Surf. Sci. 442, 1-8 (1999)

(13) J.F. Skelly, T. Bertrams, A.W. Munz, M.J. Murphy, A. Hodgson. Nitrogen induced restructuring of Cu(111) and explosive desorption of N_2. Surf. Sci. 415, 48–61 (1998)

(14) A.M. Goedken, S.L. Silva, S.M. York, F.M. Leibsle STM studies of the N/Cu(111) system: surface structure,electron confinement and tip-induced modification. Eur. Phys. J. AP 19, 77-82 (2002)

(15) H. Baek, S. Jeon, J. Seo, Y. Kuk. Geometric and Electronic Structure of Passive CuN Monolayer on Cu(111) : A Scanning Tunneling Microscopy and Spectroscopy Study. J. Korean Phys. Soc. 56 (2), 620624 (2010)

(16) A. Soon, L. Wong, M. Lee, M. Todorova, B. Delley, C. Stampfl. Nitrogen adsorption and thin surface nitrides on Cu(111) from first-principles Surf. Sci. 601, 4775–4785(2007)